

# Atom-atom correlations in colliding Bose-Einstein condensates

Magnus Ögren and K. V. Kheruntsyan

*ARC Centre of Excellence for Quantum-Atom Optics, School of Physical Sciences, University of Queensland, Brisbane, Queensland 4072, Australia*

(Received 31 July 2008; published 17 February 2009)

We analyze atom-atom correlations in the  $s$ -wave scattering halo of two colliding condensates. By developing a simple perturbative approach, we obtain explicit analytic results for the collinear (CL) and back-to-back (BB) correlations corresponding to realistic density profiles of the colliding condensates with interactions. The results in the short-time limit are in agreement with the first-principles simulations using the positive- $P$  representation and provide analytic insights into the experimental observations of Perrin *et al.* [Phys. Rev. Lett. **99**, 150405 (2007)]. For long collision durations, we predict that the BB correlation becomes broader than the CL correlation.

DOI: [10.1103/PhysRevA.79.021606](https://doi.org/10.1103/PhysRevA.79.021606)

PACS number(s): 03.75.Kk, 05.30.-d, 34.50.-s

Experiments with colliding Bose-Einstein condensates (BECs) [1,2] are currently attracting considerable attention in the field of ultracold quantum gases [3–11]. A recent breakthrough in this area is the direct detection [2] of atom-atom pair correlations in the  $s$ -wave scattering halo formed in the collision of metastable helium ( $^4\text{He}^*$ ) condensates. Experimental advances like this pose increasingly demanding challenges to theory due to the need to provide quantitatively accurate descriptions in realistic parameter regimes.

Theoretical developments are taking place on two fronts, using (i) numerical techniques based on stochastic phase-space methods (such as the first-principles simulations in the positive- $P$  representation [9,11] or approximate simulations based on the truncated Wigner-function expansion [8]), and (ii) analytic methods such as the Bogoliubov theory [5–7], undepleted source approximation [4,11], and a simple Gaussian ansatz [10]. (The analytic methods often represent extensions of quantum optics approaches describing closely related systems of parametric down-conversion and four-wave mixing [12].) Despite these developments, the existing numerical techniques still fall short of fully describing the experimental measurements of Ref. [2], whereas the approximations of the analytic methods are usually too severe to lead to full quantitative agreement with the experiments.

In this Rapid Communication, we develop an alternative analytic scheme to obtain explicit results for atom-atom correlations in condensate collisions. The scheme is rather simple, yet it compares surprisingly well with the exact positive- $P$  simulations in the short-time limit. The main advantages of the method are the analytic transparency and the fact that it can model realistic density profiles of the colliding condensates with interactions. This is important for addressing the role of mode mixing due to the inhomogeneity of trapped atomic clouds, which is the strongest effect that influences the strengths and the width of atom-atom correlations. Our results may also have implications for future experiments aimed at producing relative atom number squeezing [11,13–15] and Einstein-Podolsky-Rosen correlations [16,17].

Additionally, we perform first-principles positive- $P$  simulations of the collision dynamics and analyze the widths of the collinear (CL) and back-to-back (BB) correlations as per

measurements of Ref. [2]. These characterize, respectively, the pair correlations between the scattered atoms propagating in the same and in the opposite directions. The simulations are performed for  $^{23}\text{Na}$  atoms (instead of  $^4\text{He}^*$  used in [2]) as this case appears to have more favorable parameters for the positive- $P$  method to remain valid for long collision durations. For comparison, in the case of  $^4\text{He}^*$  [2,11], the simulation durations were much shorter than the experimental collision time due to the smaller mass and larger scattering length of  $^4\text{He}^*$  atoms. The surprising result that we find here is that the width of the BB correlation grows with time and eventually becomes larger than the width of the CL correlation. This observation is in agreement with the measured correlation widths of Ref. [11]; it is also accompanied by the reduction of the BB correlation strength below the CL correlation, which in turn implies absence of relative number squeezing in the long-time limit.

We start by considering the equations of motion describing the collision of two BECs in the Bogoliubov approximation in which the atomic field operator is split into the mean-field (MF) and fluctuating components,  $\hat{\Psi}(\mathbf{x}, t) = \Psi_{+Q}(\mathbf{x}, t) + \Psi_{-Q}(\mathbf{x}, t) + \hat{\delta}(\mathbf{x}, t)$ . Here,  $\Psi_{\pm Q}(\mathbf{x}, t)$  represent the MF amplitudes of the colliding condensates (which can be created by splitting a single stationary condensate using a Bragg pulse or Raman lasers) with mean momenta  $+Q$  and  $-Q$  along the  $x$  axis (in wave number units, in the center-of-mass frame), whereas  $\hat{\delta}(\mathbf{x}, t)$  is the fluctuating component, which is treated quantum mechanically to the lowest order in perturbation theory. The fluctuating component satisfies the equation of motion

$$i\hbar \frac{\partial \hat{\delta}(\mathbf{x}, t)}{\partial t} = -\frac{\hbar^2 \nabla^2}{2m} \hat{\delta}(\mathbf{x}, t) + 2U\Psi_{+Q}(\mathbf{x}, t)\Psi_{-Q}(\mathbf{x}, t)\hat{\delta}^*(\mathbf{x}, t), \quad (1)$$

where  $U = 4\pi\hbar^2 a/m$  is the coupling constant describing  $s$ -wave scattering interactions, with  $a$  being the scattering length. The MF components, on the other hand, satisfy the standard time-dependent Gross-Pitaevskii (GP) equation. However, if the mean kinetic energy of the colliding atoms is much larger than the interaction energy and if we restrict

ourselves to short collision times, then the MF amplitudes can be approximated by freely propagating fields [6]:  $\Psi_{\pm Q}(\mathbf{x}, t) = \sqrt{\rho(\mathbf{x})/2} \exp(\pm iQx - i\hbar Q^2 t/2m)$ . Here,  $\rho(\mathbf{x})$  is the density profile of the initial source condensate and we have additionally assumed that the center-of-mass displacements  $x \mp v_0 t$  (where  $v_0 = \hbar Q/m$  is the collision velocity) of the MF components are negligible in the short-time limit. This is justified if the displacements during the effective collision time are much smaller than the characteristic size of the colliding BECs in the collision direction. In the experiments of Ref. [2] this was indeed the case.

Substituting the expressions for  $\Psi_{\pm Q}(\mathbf{x}, t)$  into Eq. (1) and transforming to a rotating frame  $\hat{\delta}(\mathbf{x}, t) \rightarrow \hat{\delta}(\mathbf{x}, t) \exp(-i\hbar Q^2 t/2m)$ , the equation of motion for  $\hat{\delta}(\mathbf{x}, t)$  can be rewritten in a simpler form,

$$\frac{\partial \hat{\delta}(\mathbf{x}, t)}{\partial t} = i \left( \frac{\hbar \nabla^2}{2m} + \frac{\hbar Q^2}{2m} \right) \hat{\delta}(\mathbf{x}, t) - ig(\mathbf{x}) \hat{\delta}^\dagger(\mathbf{x}, t), \quad (2)$$

where  $g(\mathbf{x})$  is a spatially dependent effective coupling given by  $g(\mathbf{x}) = 2U\Psi_{+Q}(\mathbf{x}, 0)\Psi_{-Q}(\mathbf{x}, 0)/\hbar = U\rho(\mathbf{x})/\hbar$ .

Converting to Fourier space,  $\hat{\delta}(\mathbf{x}, t) = \int d\mathbf{k} \hat{a}(\mathbf{k}, t) \exp(i\mathbf{k} \cdot \mathbf{x}) / (2\pi)^{3/2}$ , yields the following equation of motion for the amplitude operator  $\hat{a}(\mathbf{k}, t)$ :

$$\frac{d\hat{a}(\mathbf{k}, t)}{dt} = -i\Delta_k \hat{a}(\mathbf{k}, t) - i \int \frac{d\mathbf{q}}{(2\pi)^{3/2}} \tilde{g}(\mathbf{q} + \mathbf{k}) \hat{a}^\dagger(\mathbf{q}, t). \quad (3)$$

Here  $\tilde{g}(\mathbf{k}) = \int d\mathbf{x} e^{-i\mathbf{k} \cdot \mathbf{x}} g(\mathbf{x}) / (2\pi)^{3/2}$  is the Fourier transform of  $g(\mathbf{x})$ ,  $\Delta_k \equiv \hbar(k^2 - Q^2)/(2m)$ , and  $k^2 = |\mathbf{k}|^2$ .

From Eq. (3) we can easily recognize the role of mode mixing in the spatially inhomogeneous treatment compared to an idealized uniform treatment. In the present inhomogeneous case, the finite width of the coupling  $\tilde{g}(\mathbf{k})$  implies that  $\hat{a}(\mathbf{k})$  couples not only to  $\hat{a}^\dagger(-\mathbf{k})$ , but also to a range of momenta around  $-\mathbf{k}$ , within  $-\mathbf{k} \pm \delta\mathbf{k}$ . The spread in  $\delta\mathbf{k}$  determines the width of atom-atom correlations with nearly opposite momenta and is ultimately related to the momentum width of the colliding BECs.

To quantify the pair correlations expected between the  $s$ -wave scattered atoms with equal but opposite momenta due to momentum conservation and between the atoms in the collinear direction due to quantum statistical effects we use Glauber's second-order correlation function

$$g^{(2)}(\mathbf{k}, \mathbf{k}', t) = \frac{\langle \hat{a}^\dagger(\mathbf{k}, t) \hat{a}^\dagger(\mathbf{k}', t) \hat{a}(\mathbf{k}', t) \hat{a}(\mathbf{k}, t) \rangle}{n(\mathbf{k}, t) n(\mathbf{k}', t)}, \quad (4)$$

which describes the density-density correlations between two momentum components  $\mathbf{k}$  and  $\mathbf{k}'$ . The normalization with respect to the product of the densities  $n(\mathbf{k}, t)$  and  $n(\mathbf{k}', t)$  ensures that  $g^{(2)}(\mathbf{k}, \mathbf{k}', t) = 1$  for uncorrelated states. The averaging is with respect to the vacuum initial state for the scattered modes.

The linearity of Eq. (3) ensures that one can apply Wick's theorem to Eq. (4) and factorize the fourth-order moment, yielding

$$g^{(2)}(\mathbf{k}, \mathbf{k}', t) = 1 + \frac{|n(\mathbf{k}, \mathbf{k}', t)|^2 + |m(\mathbf{k}, \mathbf{k}', t)|^2}{n(\mathbf{k}, t) n(\mathbf{k}', t)}. \quad (5)$$

Here,  $n(\mathbf{k}, \mathbf{k}', t) = \langle \hat{a}^\dagger(\mathbf{k}, t) \hat{a}(\mathbf{k}', t) \rangle$  and  $m(\mathbf{k}, \mathbf{k}', t) = \langle \hat{a}(\mathbf{k}, t) \hat{a}(\mathbf{k}', t) \rangle$  are the normal and anomalous densities;  $n(\mathbf{k}, t) = n(\mathbf{k}, \mathbf{k}, t)$  is the momentum distribution.

It follows from Eq. (3) and the shape of  $\tilde{g}(\mathbf{k})$  that, for sufficiently large collision momentum  $Q$  (much larger than the momentum spread of the colliding BECs), the normal density  $n(\mathbf{k}, \mathbf{k}', t)$  acquires nonzero population primarily for pairs of nearby momenta,  $\mathbf{k}' \simeq \mathbf{k}$ , while the anomalous density  $m(\mathbf{k}, \mathbf{k}', t)$  does so for pairs of momenta that are nearly opposite,  $\mathbf{k}' \simeq -\mathbf{k}$ . Accordingly, we can concentrate on the CL and BB correlations, which are denoted via  $g_{\text{CL}}^{(2)}(\mathbf{k}, \Delta\mathbf{k}, t) = g^{(2)}(\mathbf{k}, \mathbf{k} + \Delta\mathbf{k}, t)$  and  $g_{\text{BB}}^{(2)}(\mathbf{k}, \Delta\mathbf{k}, t) = g^{(2)}(\mathbf{k}, -\mathbf{k} + \Delta\mathbf{k}, t)$  and are given by

$$g_{\text{CL}}^{(2)}(\mathbf{k}, \Delta\mathbf{k}, t) = 1 + \frac{|n(\mathbf{k}, \mathbf{k} + \Delta\mathbf{k}, t)|^2}{n(\mathbf{k}, t) n(\mathbf{k} + \Delta\mathbf{k}, t)}, \quad (6)$$

$$g_{\text{BB}}^{(2)}(\mathbf{k}, \Delta\mathbf{k}, t) = 1 + \frac{|m(\mathbf{k}, -\mathbf{k} + \Delta\mathbf{k}, t)|^2}{n(\mathbf{k}, t) n(-\mathbf{k} + \Delta\mathbf{k}, t)}. \quad (7)$$

To calculate these correlation functions in the short-time limit, we proceed with the Taylor expansion in time, up to the terms of order  $t^2$  [15]:

$$\hat{a}(\mathbf{k}, t) = \hat{a}(\mathbf{k}, 0) + \left. \frac{\partial \hat{a}(\mathbf{k}, t)}{\partial t} \right|_{t=0} t + \left. \frac{\partial^2 \hat{a}(\mathbf{k}, t)}{\partial t^2} \right|_{t=0} \frac{t^2}{2} + \dots$$

The expansion is valid for  $t \ll t_0$ , where  $t_0 = 1/g(0) = 1/[U\rho(0)/\hbar]$  is the time scale [18]. Using the right-hand side of Eq. (3), this gives, up to the lowest-order terms,

$$\begin{aligned} n(\mathbf{k}, \mathbf{k}', t) &\simeq t^2 \int d\mathbf{q} \tilde{g}(\mathbf{q} + \mathbf{k}) \tilde{g}(\mathbf{q} + \mathbf{k}') / (2\pi)^3 \\ &= t^2 \int d\mathbf{x} e^{-i(\mathbf{k} - \mathbf{k}') \cdot \mathbf{x}} [g(\mathbf{x})]^2 / (2\pi)^3, \end{aligned} \quad (8)$$

$$\begin{aligned} |m(\mathbf{k}, \mathbf{k}', t)| &\simeq t |\tilde{g}(\mathbf{k} + \mathbf{k}')| / (2\pi)^{3/2} \\ &= t \left| \int d\mathbf{x} e^{-i(\mathbf{k} + \mathbf{k}') \cdot \mathbf{x}} g(\mathbf{x}) / (2\pi)^3 \right|. \end{aligned} \quad (9)$$

From these results we see that the width of the CL correlation, Eq. (6), is determined by the square of the Fourier transform of the square of the effective coupling  $g(\mathbf{x})$ . The width of the BB correlation, Eq. (7), on the other hand, is determined by the square of the Fourier transform of  $g(\mathbf{x})$ . Therefore, the CL correlation is generally broader than the BB correlation at short times.

*Thomas-Fermi (TF) parabolic density profile.* We now give explicit analytic results for the case when the initial condensate density profile is given by the ground state of the GP equation in a harmonic trap in the TF regime:  $\rho(\mathbf{x}) = \rho_0(1 - \sum_i x_i^2/R_i^2)$  for  $\sum_i x_i^2/R_i^2 < 1$  ( $i = x, y, z$ ) and  $\rho(\mathbf{x}) = 0$  elsewhere, with  $R_i$  being the TF radius along direction  $i$  and  $\rho_0$  the peak density. For definiteness, we consider CL and BB correlations for which the displacement  $\Delta\mathbf{k}$  is along one of the Cartesian coordinates, i.e.,  $\mathbf{k}' = \pm \mathbf{k} + \mathbf{e}_i \Delta k_i$ , where  $\mathbf{e}_i$  is

the unit vector in the  $k_i$  direction. The integrals in Eqs. (8) and (9) can be performed explicitly, in terms of Bessel functions  $J_\nu(z)$  [19], yielding

$$n(\mathbf{k}, \mathbf{k} + \mathbf{e}_i \Delta k_i, t) \approx \frac{8t^2 g^2(0) \bar{R}^3 J_{7/2}(\Delta k_i R_i)}{(2\pi)^{3/2} (\Delta k_i R_i)^{7/2}}, \quad (10)$$

$$|m(\mathbf{k}, -\mathbf{k} + \mathbf{e}_i \Delta k_i, t)| \approx \frac{2tg(0) \bar{R}^3 J_{5/2}(\Delta k_i R_i)}{(2\pi)^{3/2} (\Delta k_i R_i)^{5/2}}, \quad (11)$$

where  $g(0) = U\rho_0/\hbar$ , and  $\bar{R} = (R_x R_y R_z)^{1/3}$  is the geometric mean TF radius. Applying these results to  $\Delta k_i = 0$ , using  $J_\nu(z) \approx (z/2)^\nu / \Gamma(\nu+1)$  for  $z \ll 1$  ( $\nu \neq -1, -2, \dots$ ), we obtain the following results for the atomic momentum distribution and the anomalous density:  $n(\mathbf{k}, t) \approx 4t^2 g^2(0) \bar{R}^3 / 105\pi^2$  and  $|m(\mathbf{k}, -\mathbf{k}, t)| \approx tg(0) \bar{R}^3 / 15\pi^2$ . These are uniform in the short-time limit, corresponding to *spontaneous* initiation of the scattering which populates the scattering modes uniformly [6,11] without the need to strictly conserve energy. A narrow scattering shell around  $|\mathbf{k}| = Q$  forms later in time, while the uv momentum cutoff, which must be assumed for a  $\delta$ -function interaction potential, prevents the total atom number from diverging.

Substituting Eqs. (10) and (11) into Eqs. (6) and (7), and suppressing the uniform dependency on  $\mathbf{k}$ , we obtain the following explicit results for the CL and BB correlations, valid for  $t \leq t_0$ :

$$g_{\text{CL}}^{(2)}(\Delta k_i, t) \approx 1 + \frac{105^2 \pi}{2} \left( \frac{J_{7/2}(\Delta k_i R_i)}{(\Delta k_i R_i)^{7/2}} \right)^2, \quad (12)$$

$$g_{\text{BB}}^{(2)}(\Delta k_i, t) \approx 1 + \frac{105^2 \pi}{32t^2 g^2(0)} \left( \frac{J_{5/2}(\Delta k_i R_i)}{(\Delta k_i R_i)^{5/2}} \right)^2. \quad (13)$$

The CL correlation shows the Hanbury Brown and Twiss (HBT) bunching with the peak value of  $g_{\text{CL}}^{(2)}(0, t) = 2$ . The BB correlation, on the other hand, shows superbunching ( $g_{\text{BB}}^{(2)}(0, t) > 2$ ) between atom pairs with equal but opposite momenta, with the peak value  $g_{\text{BB}}^{(2)}(0, t) = 1 + 7^2 / [2^4 t^2 g^2(0)] \gg 1$  partly reflecting the fact that typical mode occupation numbers in this spontaneous scattering regime are much smaller than 1. From the above results we also determine the widths of the CL and BB correlations, which are defined for simplicity as the half width at half maximum,  $w_i^{(\text{CL})} \approx 1.23w_i^{(\text{S})}$  and  $w_i^{(\text{BB})} \approx 1.08w_i^{(\text{S})}$ , giving the ratio of  $w_i^{(\text{CL})}/w_i^{(\text{BB})} \approx 1.14$ . Here  $w_i^{(\text{S})} \approx 1.99/R_i$  is the width of the momentum distribution  $\tilde{\rho}(k_i) = |\int d\mathbf{x} \sqrt{\rho(\mathbf{x})} \exp(-ik_i x_i) / (2\pi)^{3/2}|^2$  of the source condensate along direction  $i$ :

$$\tilde{\rho}(k_i) = \frac{\pi \rho_0 \bar{R}^6}{2} \frac{|2J_1(k_i R_i) - k_i R_i J_0(k_i R_i)|^2}{(k_i R_i)^6}. \quad (14)$$

The ratio of  $w_i^{(\text{CL})}/w_i^{(\text{BB})} \approx 1.14$  for the TF parabolic density profile (which can be contrasted with the larger value of  $\sigma_i^{(\text{CL})}/\sigma_i^{(\text{BB})} = \sqrt{2}$  in the case of a Gaussian profile; see below) is in good agreement with the results of positive- $P$  simulations of  $^4\text{He}^*$  BEC collisions for relatively short collision times ( $\lesssim 25 \mu\text{s}$ ) [11], for which the obtained ratios ranged

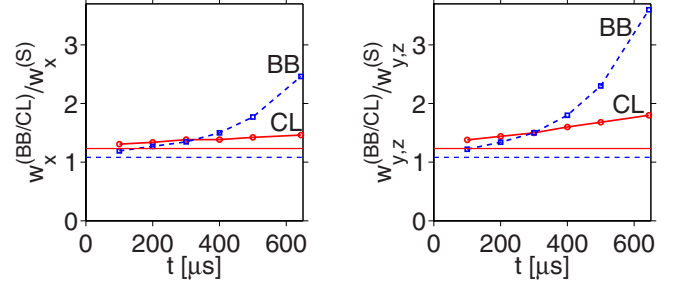


FIG. 1. (Color online) Momentum widths of the BB and CL correlations relative to the width of the source BEC in  $x$ ,  $y$ , and  $z$  directions as a function of time. The solid and dashed curves with marks are the results of the positive- $P$  simulations for  $^{23}\text{Na}$  BECs as in Ref. [9]. The horizontal solid and dashed lines are the corresponding correlation widths from Eqs. (12) and (13).

between 1.08 and 1.13 depending on the correlation direction  $i$ . Similarly, good agreement is obtained when comparing the individual widths, in which case the positive- $P$  results were  $w_x^{(\text{CL})} \approx 1.27w_x^{(\text{S})}$ ,  $w_{y,z}^{(\text{CL})} \approx 1.57w_{y,z}^{(\text{S})}$ ,  $w_x^{(\text{BB})} \approx 1.18w_x^{(\text{S})}$ , and  $w_{y,z}^{(\text{BB})} \approx 1.39w_{y,z}^{(\text{S})}$ . The somewhat larger values of the  $y, z$  correlation widths than the above analytic results are explained by the fact that the simulated source condensates were confined in the transverse ( $y$  and  $z$ ) directions much more strongly than in the axial ( $x$ ) direction, and therefore the actual GP ground-state profile (which was used as the initial condition) along  $y$  and  $z$  was intermediate between a Gaussian and a TF parabola.

The present analytic results and the positive- $P$  results for  $^4\text{He}^*$  [11] are generally in satisfactory agreement with the experimentally measured absolute widths [2], except that the experimentally measured CL width was somewhat smaller than the BB width, which is in contrast to the above analytic results and the positive- $P$  results for  $^4\text{He}^*$ . An obvious suspect for this discrepancy is the fact that the effective collision time in the experiment was  $\sim 150 \mu\text{s}$ , whereas the positive- $P$  simulations of Ref. [11] were restricted to  $\lesssim 25 \mu\text{s}$  due to the large sampling errors developed past that time. Therefore, to explain this discrepancy it is important to perform first-principle simulations for longer collision durations and monitor the long-time dynamics of the correlation widths.

To this end we have been able to perform such simulations for collisions of  $^{23}\text{Na}$  BECs, in which case the smaller scattering length and larger mass compared to  $^4\text{He}^*$  give more favorable parameter values for the positive- $P$  simulations and allow us to extend them to collision durations  $\lesssim 650 \mu\text{s}$ . More specifically, we have performed the simulations as in Ref. [9], starting from the full effective field-theory Hamiltonian, and extracted the CL and BB correlation widths as a function of time. The results are shown in Fig. 1, where the marked solid and dashed curves refer to the numerically obtained CL and BB widths, respectively. The horizontal solid and dashed lines, on the other hand, are the corresponding CL and BB widths from the present analytic treatment, Eqs. (12) and (13). We see that the short-time asymptotic limits of the exact numerical results converge to the analytic predictions, thus proving the validity and usefulness of the developed analytic approach in this limit.

The long-time dynamics of the correlation widths from the positive- $P$  results show that at some point in time the BB correlation width becomes larger than the CL width. This supports the experimental observations of Ref. [2] that  $w_{y,z}^{(\text{BB})} > w_{y,z}^{(\text{CL})}$ . It is interesting to note that the crossover point ( $\sim 300 \mu\text{s}$ ) is close to the point in time ( $\sim 400 \mu\text{s}$ ) where the peak BB correlation drops below the collinear HBT peak value of 2 (see Fig. 3(a) of [9]). Both these observations seem to be unique to the exact first-principle simulations and have not been observed so far using approximate theoretical techniques. We attribute these effects to the dynamical broadening of the momentum distributions of the expanding condensates, and partly to rescattering of scattered atoms with opposite momenta back into the condensate modes.

The importance of the observation of  $g_{\text{BB}}^{(2)}(0, t) < g_{\text{CL}}^{(2)}(0, t)$  is related to the prospect of observing relative number squeezing between the  $s$ -wave scattered atoms with equal but opposite momenta [11]. The relative number squeezing itself is a manifestation of a violation of the classical Cauchy-Schwartz inequality, corresponding to  $g_{\text{BB}}^{(2)}(0, t) > g_{\text{CL}}^{(2)}(0, t)$  [14], while the opposite inequality corresponds to absence of squeezing. While we certainly do have a violation and relative number squeezing in the short-time limit [11], the above observation that  $g_{\text{BB}}^{(2)}(0, t)$  becomes smaller than  $g_{\text{CL}}^{(2)}(0, t)$  implies that the squeezing is lost for long collision durations.

*Gaussian density profile.* We now give the results for a Gaussian density profile of the source condensate,  $\rho(\mathbf{x}) = \rho_0 \exp(-\sum_i x_i^2 / 2\sigma_i^2)$ , corresponding to the momentum distribution of  $\tilde{\rho}(\mathbf{k}) \propto \exp(-\sum_i k_i^2 / 2\sigma_{k_i}^2)$ , where  $\sigma_i$  and  $\sigma_{k_i} = 1/2\sigma_i$

are the rms widths. Following the same procedures as with the TF parabola, we obtain

$$g_{\text{CL}}^{(2)}(\Delta k_i, t \ll t_0) \simeq 1 + \exp(-\Delta k_i^2 / 8\sigma_{k_i}^2), \quad (15)$$

$$g_{\text{BB}}^{(2)}(\Delta k_i, t \ll t_0) \simeq 1 + \frac{8}{t^2 g^2(0)} \exp(-\Delta k_i^2 / 4\sigma_{k_i}^2). \quad (16)$$

The correlation widths are now given by  $\sigma_{k_i}^{(\text{CL})} = 2\sigma_{k_i}$  and  $\sigma_{k_i}^{(\text{BB})} = \sqrt{2}\sigma_{k_i}$ , resulting in the ratio  $\sigma_{k_i}^{(\text{CL})} / \sigma_{k_i}^{(\text{BB})} = \sqrt{2}$ . These results are in agreement with those of Ref. [10] (and Ref. [6] under the same approximations as here) and represent an alternative derivation in the Gaussian case.

In summary, we have developed a simple perturbative approach to pair correlations between the atoms scattered from a collision of two BECs. The analytic results obtained show how the CL and BB correlations depend on the shape and the size of the colliding condensates. The results are compared with exact positive- $P$  simulations and are in good agreement in the short time limit. The long-time dynamics—accessible through the positive- $P$  simulations of sodium condensates—give evidence that the BB correlation width grows with time faster than the CL correlation width and that it can become broader than the CL width. This conclusion agrees with the experimental observation of Ref. [2], in contrast to previous theoretical predictions.

The authors acknowledge support from the Australian Research Council and thank A. Aspect, C. I. Westbrook, D. Boiron, K. Mølmer, P. Deuar, M. Trippenbach, P. Ziñ, and J. Chwedeñczuk for stimulating discussions.

- 
- [1] J. M. Vogels, K. Xu, and W. Ketterle, Phys. Rev. Lett. **89**, 020401 (2002).
  - [2] A. Perrin *et al.*, Phys. Rev. Lett. **99**, 150405 (2007).
  - [3] Y. B. Band *et al.*, Phys. Rev. Lett. **84**, 5462 (2000).
  - [4] V. A. Yurovsky, Phys. Rev. A **65**, 033605 (2002).
  - [5] R. Bach, M. Trippenbach, and K. Rzażewski, Phys. Rev. A **65**, 063605 (2002).
  - [6] P. Ziñ, J. Chwedeñczuk, and M. Trippenbach, Phys. Rev. A **73**, 033602 (2006).
  - [7] J. Chwedeñczuk *et al.*, Phys. Rev. A **78**, 053605 (2008).
  - [8] A. A. Norrie, R. J. Ballagh, and C. W. Gardiner, Phys. Rev. Lett. **94**, 040401 (2005).
  - [9] P. Deuar and P. D. Drummond, Phys. Rev. Lett. **98**, 120402 (2007).
  - [10] K. Mølmer *et al.*, Phys. Rev. A **77**, 033601 (2008).
  - [11] A. Perrin *et al.*, New J. Phys. **10**, 045021 (2008).
  - [12] D. F. Walls and G. J. Milburn, *Quantum Optics*, 2nd ed. (Springer, Berlin, 2008).
  - [13] C. M. Savage, P. E. Schwenn, and K. V. Kheruntsyan, Phys. Rev. A **74**, 033620 (2006).
  - [14] C. M. Savage and K. V. Kheruntsyan, Phys. Rev. Lett. **99**, 220404 (2007).
  - [15] M. Ögren and K. V. Kheruntsyan, Phys. Rev. A **78**, 011602(R) (2008).
  - [16] H. Pu and P. Meystre, Phys. Rev. Lett. **85**, 3987 (2000).
  - [17] K. V. Kheruntsyan, M. K. Olsen, and P. D. Drummond, Phys. Rev. Lett. **95**, 150405 (2005).
  - [18] With this expansion, the commutation relation is given by  $[\hat{a}(\mathbf{k}, t), \hat{a}^\dagger(\mathbf{k}', t)] \approx \delta(\mathbf{k} - \mathbf{k}')$  up to terms of order  $t^2$ .
  - [19] A. Erdelyi, W. Magnus, F. Oberhettinger, and F. G. Tricomi, *Higher Transcendental Functions* (McGraw-Hill, New York, 1953), Vol. 2.